16th European Signal Processing Conference (EUSIPCO 2008), Lausanne, Switzerland, August 25-29, 2008, copyright by EURASIP

GEOMETRICAL FEATURE EXTRACTION FROM ULTRASONIC TIME FREQUENCY IMAGES: AN APPLICATION TO NONDESTRUCTIVE TESTING OF MATERIALS

Ramon Miralles, Soledad Gomez, Valery Naranjo and Addisson Salazar

Instituto de Telecomunicaciones y Aplicaciones Multimedia (iTEAM), Dpto. de Comunicaciones,
Universidad Politécnica de Valencia (U.P.V.)
Camino de Vera S/N, 46022, Valencia, Spain
phone: +3496 3879737, fax: +3496 3877309, email: rmiralle@dcom.upv.es
web: www.gts.upv.es

ABSTRACT

Signal processing of ultrasonic scans is frequently used for material classification. Extracted parameters from the ultrasonic registers are used in statistical classification algorithms. There are situations where interactions taking place inside the material are so complex that the number of significative parameters is not enough to get good classification percentages. What we propose in this work is to use geometrical parameters extracted from the time frequency representation of the ultrasonic register in this situations. The presented technique merges some ideas of nondestructive testing of materials and image descriptors to get an easy to implement algorithm that could be applied in many different products and situations.

1. INTRODUCTION

Signal processing of ultrasonic signals is frequently used in nondestructive testing (NDT) of materials. Many physical and mechanical properties can be extracted from the ultrasonic registers. Although there are some situations where very little signal processing is needed, there are some other where extracting these properties is a complex task. Characterization of scattering materials is a good example where intensive signal processing is needed. Due to the high attenuation of this kind of materials, pulse-echo inspection (similar to radar operation) is frequently used. Typical parameters extracted for characterization are: attenuation, longitudinal velocity, central or centroid frequency evolution with depth, bandwidth, etc. Applications that can get benefits from these studies are of special relevance. We can mention medical characterization of tissues [1], construction industry [2], alimentary industry [3], etc.

In this work we will analyze the possibility of extracting characterization parameters from a different point of view. We work with binarized time frequency representation (TFR) of ultrasonic recorded signals as if they were images. If a human operator was inspecting this images for material classification he would soon realize that there were some shape related parameters strongly correlated with material categories. This work shows how geometrical related parameters can be extracted for characterization/detection in nondestructive testing of materials. The main advantage of this strategy is that it is less related to physical phenomena taking place in NDT than typical strategies and it can be employed even when very little knowledge is available.

This work is going to be structured as follows. In section 2 we will describe the ultrasonic registers obtained in scattering materials by means of an approximated model. Later, in section 3, we will study the effect of the observation noise when binarizing the TFR and the image descriptors employed. In section 4 we will show an example of how the proposed technique can be used. Finally in section 5, conclusions and future work will be presented.

This work was supported by the national R+D program under grant TEC2005-01820/TCM (Spain) and by the Spanish MEC in the FPU program.

2. ULTRASONIC PULSE MODELLING IN THE FREQUENCY DOMAIN

The starting point of our analysis will be an ultrasonic transducer inspecting in pulse-echo mode a given scattering material. It is very frequently assumed that the emitted ultrasonic pulse can be frequency modelled with a Gaussian envelope [4, 5] (see equation (1)).

$$S(\omega) = A \cdot e^{\frac{-(\omega-\omega_c)^2}{B^2}} \tag{1}$$

.

The parameters ω_c and B are, respectively, the transducer central pulsation and bandwidth.

The ultrasonic pulse, as it travels through the material, suffers attenuation due to different phenomenas (absorption, scattering, etc.). Many of this phenomenas can be modelled by means of power-law approximations [6, 7]. As an example we can see the power law that governs the attenuation of many soft tissues:

$$\alpha_s(\omega) = e^{-\alpha_0 \cdot \omega^y \cdot z} \tag{2}$$

The parameters α_0 and y are tissue dependent attenuation parameters. In general, the exponent that controls the power law is in the range $1 \leq y \leq 2$ [4]. Using equation (1) and equation (2) we can formulate the spectra of the ultrasonic pulse after it travels z into the material as seen in equation (3).

$$S(\omega, z) = A \cdot e^{\frac{-(\omega-\omega_c)^2}{B^2}} \cdot e^{-\alpha_0 \cdot \omega^y \cdot z} \tag{3}$$

.

For $y = 1$ or $y = 2$ equation (1) can be demonstrated to be equal to:

$$S_g(\omega,z) = \overline{A}(z)\cdot e^{\frac{-(\omega-\overline{\omega_c}(z))^2}{\overline{B}^2(z)}} \quad (4)$$

,

with $\overline{A}(z)$, $\overline{\omega_c}(z)$ and $\overline{B}(z)$ the new amplitude, central pulsation and bandwidth that take into account the tissue dependent attenuation parameters (see [4] for a complete derivation of this values). When $1 < y < 2$ the formulation is more complex and in general it does not exactly follow a Gaussian envelope. However, it can be empirically demonstrated that Gaussian approximation in this situation is quite accurate. Figure 1 shows the amplitude normalized maximum error with the Gaussian approximation. Figure 1 was simulated for a f_c=250 KHz central frequency ultrasonic pulse with initial bandwidth B=100 KHz that propagates with the law defined in equation (3) up to z=3 cm.

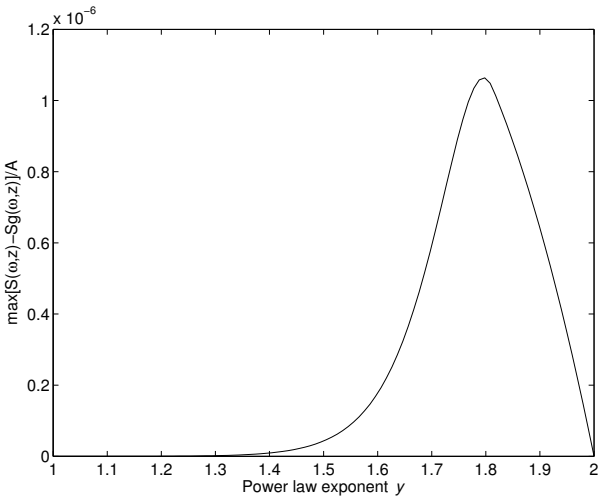

Figure 1: Amplitude normalized maximum error obtained in Gaussian approximation.

The TFR of a register obtained in NDT of scattering materials can be modeled using equation (4). The parameters $\overline{A}(z)$, $\overline{\omega_c}(z)$ and $\overline{B}(z)$ will affect the shape of the TFR and, of course, of the binarized TFR.

Conventional techniques frequently used for material classification are based on extracting parameters directly from the ultrasonic register [5, 8]. In the next section we are going to present a complimentary parameter extraction when processing TFR as images.

3. AN ALTERNATIVE TECHNIQUE TO CONVENTIONAL PARAMETER EXTRACTION FOR MATERIAL CHARACTERIZATION

Ultrasonic signals obtained in nondestructive testing of scattering materials are frequently modelled as time varying signals. The selective attenuation of the materials is among some other phenomenas responsible of that. Classical stationary parameter extraction algorithms are not valid in this situation. A possible alternative is to assume slow variation of the signal statistics and work with an sliding window [9] or with a time frequency representation (TFR) [10]. What we propose in this work is to transform the TFR in a binarized image (we will later see how to fix the threshold) and extract geometrical parameters using image processing algorithms.

The underlying idea on this approximation is to extract geometrical parameters with a physical meaning very closed related to what a human operator expects when inspecting TFR diagrams. For instance, the model presented in equation (3), predicts a down-shift in the center frequency and a narrowing bandwidth for materials obeying this law. In this case we could think of extracting geometrical image parameters related to curvature of a given shape, rotation or even eccentricity.

An adequate threshold selection should be done before binarizing the TFR image. If we assume that the ultrasonic signal recorded is contaminated by additive white Gaussian noise (AWGN), the binarized TFR will exhibit some sort of two-dimensional 'jitter'. This jitter will affect the shape of the binarized TFR and, of course, the geometrical parameters derived from it. The figure 2 shows the contour of the binarized TFR without AWGN (solid line) and the binarized TFR when AWGN of variance 0.17 is added (grey area limited by the dashed line represent the uncertainty area produced by noise) when a constant threshold in all TFR is applied. An alternative when trying to minimize the effect of noise is to use variable with depth threshold value. In this case the binarizing threshold will be fixed at the level where the Gaussian envelope slope is maximum (see figure 3). It can be observed in the figures 2 and 3 that variable threshold works better if the amplitude of the Gaussian envelope is higher than noise whereas constant threshold is better for noise comparable amplitudes. What we propose in this work is to combine both thresholds into a single one (figure 4). We first estimate the depth where the noise energy level is comparable to ultrasonic component energy (z_0). Then, variable threshold at maximum slope is used up to (z_0). After this depth constant threshold is applied.

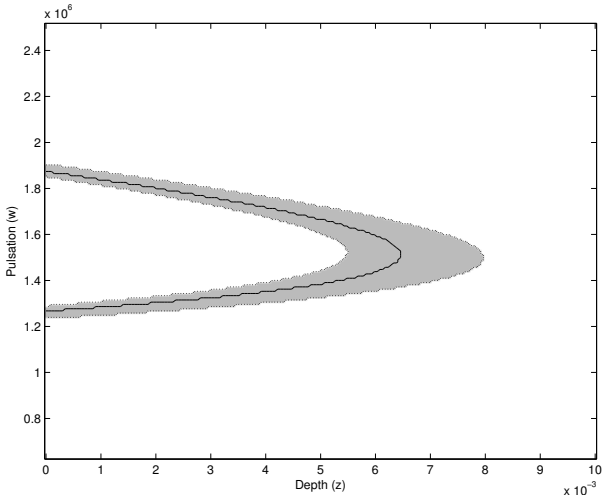

Figure 2: Simulation of the model presented in equation (3) for the power law with $y = 2$ (constant threshold). Binarized TFR image with AWGN of variance 0.17.

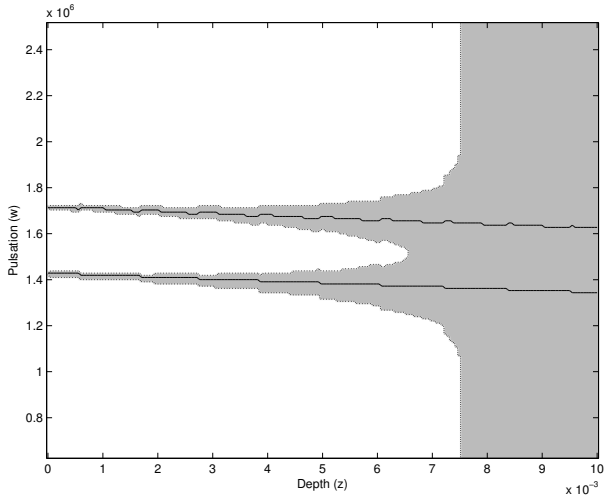

Figure 3: Simulation for the power law with $y = 2$ (variable threshold). Binarized TFR image with AWGN of variance 0.17.

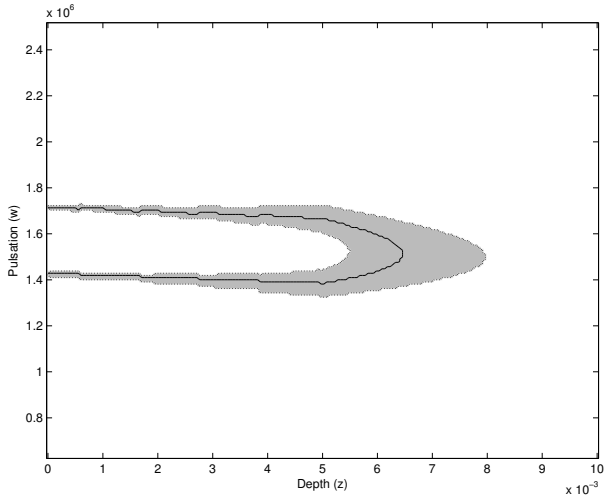

Figure 4: Simulation for the power law with $y = 2$ (mixed threshold). Binarized TFR image with AWGN of variance 0.17.

3.1 Image Descriptors

Let us call $I(z,\omega)$ the binarized TFR generated with the mixed threshold previously described. We can calculate many geometrical descriptors [11]. Our contribution, at this point, is to work with image processing parameters having a physical meaning related to the expected changes produced in the TFR. It is expectable that geometrical descriptors will let us a most intuitive representation of the model in comparison with the classical signal processing parameters. For example, we can establish visual relations between orientation parameters and physical variations of attenuation or bandwidth along depth. The most representative geometrical descriptors we work with are:

1. **Area:**
   For a generic discrete function in two variables, the moments are defined as:

$$m_{pq} = \sum\sum z^p \omega^q I(z,\omega) \tag{5}$$

   where $I(z,\omega)$ is the binarized TFR, at coordinates (z,ω). The area can be obtained as the zero-order moment $m_{00} = \sum\sum I(z,\omega) \equiv Area$. The area is related to attenuation parameters. For a similar scatterer density, materials with higher attenuation parameters get lower area descriptors.
2. **Center of gravity:** The center of gravity or centroid of a binary image can be calculated by using first-order moments. Being $m_{10} = \sum\sum z \cdot I(z,\omega)$ and $m_{01} = \sum\sum \omega \cdot I(z,\omega)$ we can define the center of mass as (c_z, c_ω) where:

$$c_z = \frac{m_{10}}{m_{00}} \quad \text{and} \quad c_\omega = \frac{m_{01}}{m_{00}} \tag{6}$$

   .
   By dividing the binary image in smaller regions, along z axis, we will be able to study the central frequency evolution with depth. Moreover, the center of gravity is used in the definition of the second-order moments as described in equation 7, note the invariance with respect to image scaling.

$$\mu_{pq} = \frac{1}{m_{00}} \sum\sum (z - c_z)^p (\omega - c_\omega)^q I(z,\omega) \tag{7}$$

3. **Orientation:** Object orientation (ϕ) can be calculated using second-order moments. It is geometrically described as the angle between the major axis of the object and the axis z. By minimizing the function $S(\phi) = \sum\sum[(z - c_z)cos\phi - (\omega - c_\omega)sin\phi]^2$ we get the next expression for the orientation:

$$\phi = \frac{1}{2} arctan\left(\frac{2\mu_{11}}{\mu_{20} - \mu_{02}}\right) \tag{8}$$

4. **Eccentricity:** Another important parameter derived from second-order moment is the eccentricity, ε. The eccentricity allows to estimate how similar to a circle an object is. The value ranges from 0 to 1 ($0 < \varepsilon < 1$). Small eccentricity values correspond to elliptical shapes while values close to 1 correspond to circular ones. For low attenuation materials eccentricity is expected to be lower than for high attenuation materials for a similar scatterer density.
5. **Signature:** A signature is a 1-D representation of an object boundary. One of the most simple ways to generate a signature is to plot the distance from the center of gravity of the region to the boundary as a function of angle (see figure 5). The changes in size of a shape results in changes in the amplitude values of the corresponding signature. It is expected that the higher the attenuation is, the lower the amplitude of the corresponding signature. Moreover, signatures not only provides information about area changes but also provides the angular direction of such changes. To compute the signature we need to compute for each angle, θ, the Euclidean distance between the center of gravity and the boundary of the region. As will be demonstrated, it is expectable that different values of the attenuation coefficient, for the model or material under test, will correspond with different signatures for the binary TFR.

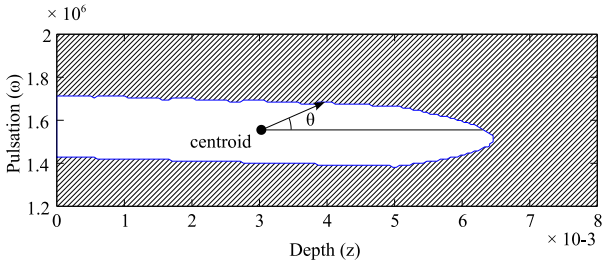

Figure 5: Signature descriptor

		Area	Orientation	Eccentricity
0% Salt	test piece 1	323	0.26	0.48
	test piece 2	404	0.04	0.38
3.5% Salt	test piece 3	219	-0.06	0.60
	test piece 4	203	-0.51	0.79

Table 1: Area, orientation and eccentricity image descriptors on the four test pieces.

4. EXPERIMENTS

Experiments were performed on four test pieces made from a matrix material of gelatine substance containing bubbles and salt (ClNa) in different concentrations. Construction of the test pieces was done as follows: in the first set of two test pieces we employed distilled water with gelatine concentration of 5%. For the second set we employed distilled water with salt concentration of 3.5% and gelatine concentration of 5%. The addition of salt increases the ultrasonic attenuation with respect to distilled water of the test pieces. In both sets we produced bubbles by stirring when the gel was sufficiently viscous. Care was taken to obtain uniform distribution of bubbles. Figure 8 shows the aspect of a test piece.

An ultrasonic PC board IPR-100 (Physical Acoustics) with 400 V of attack voltage, 40 dB in the receiver amplifier and damping impedance of 2000 Ohms was used. The transducer frequency was chosen to be 1MHz (K1SC transducer probe from Krautkramer & Branson). Received signal was acquired with the Tektronix 3000 oscilloscope (f_s=50 MSamples/s).

Uniformly distributed a-scans were obtained around the test piece contour. Individual a-scan TFRs were obtained using the Spectrogram (by means of the Short Time Fourier Transform). Final TFR for each test piece was obtained averaging individual a-scan TFRs. After thresholding the final TFR, geometrical descriptors presented in section 3 were calculated for each test piece.

The table 1 shows the area, orientation and eccentricity for the test pieces created in the experiment. As it was expected values obtained are similar for test pieces with equal salt concentration. Area and eccentricity values obtained agree with the expected behavior described in section 3.

In figure 6 we can see the signature as it was defined in previous section. Again, similar behavior is obtained for test pieces with equal salt concentration. Analogous results are obtained in figure 7 for the central frequency evolution calculated from geometrical image descriptors.

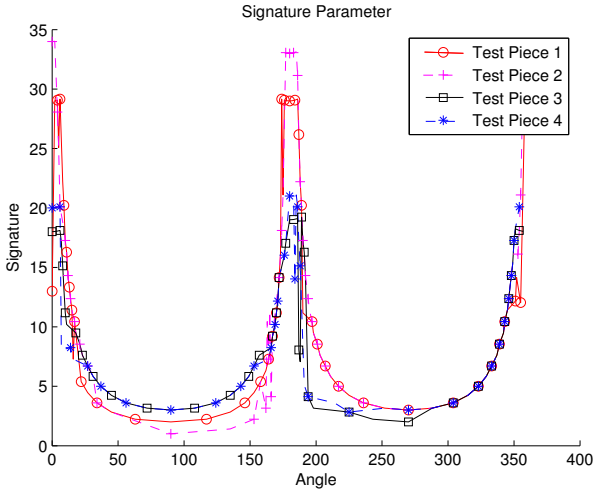

Figure 6: Signature descriptor

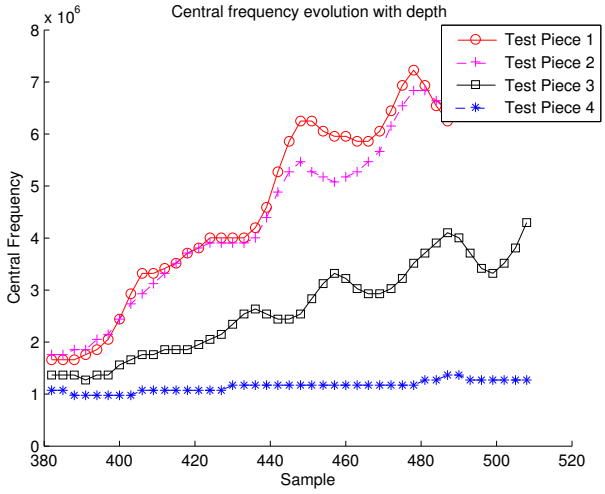

Figure 7: Center frequency evolution with depth

5. CONCLUSIONS AND FUTURE WORK

In this work we show that parameters extracted from the TFR of ultrasonic a-scans can be used for material characterization/ classification. The novelty of this work is based on the use of TFR as input images in image processing algorithms, specifically image descriptors. We do not intend to substitute traditional extracted parameters directly form the a-scans. This technique was devised to compliment traditional classification parameters (attenuation, longitudinal ultrasonic velocity,...) with shape related parameters typically used in image processing.

In order to show that material parameters affect the shape of the TFR we have employed a simple power-law polyno-

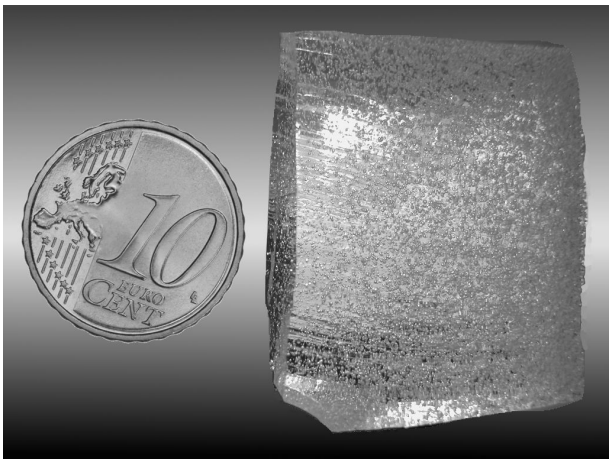

Figure 8: Fragment of a test piece

mial model with Gaussian envelope assumption. We have proven by simulations the accuracy of the Gaussian envelope approximation.

Early results are promising when using the TFR image for material classification. We have seen in a real experiment the ability of the image descriptors to distinguish between two different scattering materials by means of ultrasonic inspection. However, further comparative work is needed to quantitatively obtain the degree of improvement of classification algorithms when using image descriptors based parameters.

REFERENCES

[1] K.K. Shung and G.A. Thieme. *Ultrasonic Scattering in Biological Tissues*. CRC, N.W. Boca Raton, Florida, 1992.

[2] L. Vergara, R. Miralles, J. Gosalbez, J.V. Fuente, U.L. Gómez, J.JAnaya, M.G. Hernández, and M.A. Izquierdo. On estimating concrete porosity by ultrasonic signal processing techniques. In *17th ICA*, Roma, September 2001.

[3] M.J.W. Povey. *Rapid Determination of Food Material Properties, Ultrasound in Food Processing*. Blackie Academic & Professional, London, Wenheim, New York, 1997.

[4] Ping He. Simulation of ultrasound pulse propagation in lossy media obeying a frequency power law lossy media obeying a frequency power law. *ieee transactions on ultrasonics, ferroelectrics, and frequency control*, 45(1):114–125, January 1998.

[5] R. Demirli and J. Saniie. Model-based estimation of ultrasonic echoes part i: Analysis and algorithms. *ieee transactions on ultrasonics, ferroelectrics, and frequency control*, 48(3):787–802, May 2001.

[6] M. Karaoguzt, N. Bilgutay, and B. Onarafl. Modeling of scattering dominated ultrasonic attenuation using power-law function. *IEEE Ultrasonic Symposium*, 1:793–796, October 2000.

[7] K.R. Waters, M.S. Hughes, J. Mobley, G.H. Brandenburger, and J.G. Miller. On the applicability of kramer-skroonig relations for ultrasonic attenuation obeying a frequency power law. *J. Acoust. Soc. Am.*, 108(2):556–563, August 2000.

[8] L. Vergara, J. Gosalbez, J.V. Fuente, R. Miralles, I. Bosch, A. Salazar, A.M. Lopez, and L.E. Dominguez. Ultrasonic nondestructive testing on marble rock blocks. *Materials Evaluation*, 62(1):73–78, January 2004.

[9] A. Salazar, R. Miralles, A. Parra, L. Vergara, and J. Gosalbez. Ultrasonic signal processing for archaeological ceramic restoration. pages 1–4, Toulouse, Francia, 2006. ICASSP 2006.

[10] J. Gosalbez, A. Salazar, I. Bosch, R. Miralles, and L. Vergara. Application of ultrasonic nondestructive testing to the diagnosis of consolidation of a restored dome. *Materials Evaluation*, 64(5):492–497, 2006.

[11] I. Pitas. *Digital Image Processing Algorithms and Applications*. Wiley-Interscience; 1 edition, February 2000.